Subsonic Airfoils with a Given Pressure Distribution

A. Hassan*
Arizona State University, Tempe, Arizona
H. Sobieczky†
DFVLR, Göttingen, Federal Republic of Germany
and
A. R. Seebass‡
University of Colorado, Boulder, Colorado

An inverse design procedure for subcritical airfoils, based on hodograph techniques, has been developed. For the subcritical flows considered here, the pressure distribution is prescribed. In the special variables used, the equation for the stream function is solved iteratively using a fast Poisson solver. The results are then mapped back to the physical plane to determine the airfoil shape. Examples of subcritical airfoil designs are presented. They show good agreement with the direct computation of the flow past the designed airfoil.

Introduction

HISTORICALLY, the analysis and design of two-dimensional airfoil sections have been treated as two distinct problems. In the former a section geometry is chosen and its aerodynamic characteristics, such as lift, drag, and moment coefficients, are determined. In the latter a section geometry is sought which will exhibit certain desirable properties. It is well known that many desirable requirements for the flow of air past a surface (e.g., delay of transition or separation of the boundary layer) may be met by imposing certain conditions on the velocity distribution along the surface.[1] The ability to design airfoils that will provide a given pressure distribution is therefore highly desirable.

Goldstein's[2] theory of thin airfoils achieves this, but the limitation to thin airfoils restricts its application. The exact theory of Theodorsen on which it is based used to be prohibitively long even for the direct problem, i.e., the calculation of the velocity distribution from a given airfoil geometry. Presumably modern symbol manipulation schemes, such as MACSYMA, could alleviate this difficulty somewhat. Major progress has been made in the analysis of airfoil sections (in particular transonic airfoils) by Sells,[3] Murman and Cole,[4] Garabedian and Korn,[5], and Jameson.[6] A parallel effort has also addressed the design problem.

Recently, there have been a number of successful attempts to develop numerical solution procedures for the "inverse" problem, i.e., design problem, in compressible flow. The design procedure developed by Volpe and Melnik[7] follows Lighthill's[8] formulation in using a computational plane based on a conformal map of the airfoil to a circle. In their method, which is based on solving the full nonconservative potential equation, they introduce three free parameters in the target pressure distribution. These parameters are adjusted during the computation to assure the existance of a solution to the inverse problem as well as to satisfy specified trailing-edge closure conditions. In the method of Tranen,[9] an iterative procedure, which is a sequence of solutions to the inverse and direct problems, is utilized to generate airfoil geometries that satisfy the input target pressures. In the method of Nixon,[10] airfoil designs were obtained by considering prescribed pressures that were small modifications of pressure distributions taken from direct solutions. Other methods of airfoil design that are based on iterated solutions of the direct problem include those of Hicks and Vanderplaats[11] and Davis.[12] In these methods direct solutions are sought with an airfoil shape that is modified in an iterative procedure to minimize the difference between the computed pressures and the prescribed target pressure distribution. More recently, these methods were successfully extended for the design of finite wings (e.g., see Haney and Johnson[13] and Hicks and Henne[14]).

Hodograph design methods were developed by Niewland,[15] Bauer, Garabedian, and Korn,[16] Boerstoel and Huizing,[17] and Sobieczky.[18] Niewland developed a technique for computing quasielliptic airfoil sections. His technique constructs a solution from a linear combination of solutions to the hodograph equation for the stream function. The solutions are found, of course, by separation of variables. The design procedure developed by Garabedian et al. uses the method of complex characteristics and is mathematically elegant. However, even in its user-oriented version, practical use of the method requires much experience and mathematical insight. Nevertheless, some very useful shock-free supercritical airfoil sections were found. These have served us well as examples for various analysis codes as well as for extensive airfoil design studies. Boerstoel and Huizing also provided shock-free supercritical airfoils using a linear combination of simple compressible flow solutions for the two-sheeted hodograph surface of lifting flows. Another indirect approach was developed by Sobieczky. Here the rheoelectric analogy[19] to the compressible flow equations was used to define a number of transonic airfoil flows.

The design procedure developed here is an improvement of the above method. Since the use of an electrical setup, of course, did not provide for economical use of the method, it did lead to a greater understanding of this indirect approach. By replacing the electric analog with a fact elliptic solver, we could use all the experience of the analog method concerning the boundary conditions that result in interesting airfoil designs. While the procedure is capable of handling both shock-free supercritical as well as subcritical airfoil sections,

Presented as Paper 81-1235 at the AIAA 14th Fluid and Plasma Dynamics Conference, Palo Alto, Calif., June 23-25, 1981, submitted May 10, 1982, revision received Oct. 6, 1983.

*Assistant Professor, Mechanical and Aerospace Engineering Department. Member AIAA.
†Research Scientist.
‡Dean, College of Engineering and Applied Sciences. Fellow AIAA.

only subcritical airfoils are discussed in this paper (the transonic airfoil design problem will be addressed in a future publication). The method requires less than a minute of CYBER 175 CPU time for the design of a subcritical airfoil section. Although the method is limited to two-dimensional flow, it does allow the user to specify a desired pressure distribution and to achieve it with little difficulty through an iterative process.

It should be mentioned that the primary goal of this research was to demonstrate through many numerical examples that the method accurately determines the airfoil shape corresponding to an input target pressure. This goal, however, dictated that we compare our results with those obtained from a direct computation of the flow past the designed airfoil rather than with those obtained from an alternative design method.

Formulation

Basic Equations

The mathematical formulation of the problem assumes a steady, two-dimensional, irrotational flow of a perfect gas. The basic equations of motion are

$$\nabla \cdot \rho q = 0 \tag{1}$$

$$\nabla \times q = 0 \tag{2}$$

and

$$p/\rho^{\gamma} = \text{const} \tag{3}$$

We satify Eq. (1) by introducing the usual stream function ψ,

$$\psi_y = \rho u = \rho q \cos(\theta)$$

$$\psi_x = -\rho v = -\rho q \sin(\theta) \tag{4}$$

and Eq. (2) by defining a potential function ϕ, such that

$$\nabla \phi = q$$

or

$$u = \phi_x, \qquad v = \phi_y \tag{5}$$

Equations (4) and (5) can be combined to give

$$\phi_x = (1/\rho)\psi_y$$

$$\phi_y = -(1/\rho)\psi_x \tag{6}$$

which can be reduced to a single equation in either ϕ or ψ, viz.,

$$\psi_{xx} + \psi_{yy} = \left(\frac{\rho_x}{\rho}\right)\psi_x + \left(\frac{\rho_y}{\rho}\right)\psi_y$$

$$\phi_{xx} + \phi_{yy} = -\left(\frac{\rho_x}{\rho}\right)\phi_x - \left(\frac{\rho_y}{\rho}\right)\phi_y \tag{7}$$

with

$$\rho = \rho(q), \qquad q = |\nabla \phi| \tag{8}$$

Equations (7) are elliptic for $M<1$ (subsonic flow), hyperbolic for $M>1$ (supersonic flow), and parabolic where $M=1$ (sonic flow). To solve either of Eqs. (7) two boundary conditions must be provided. The first of these represents the behavior of the flow in the far field and the second the flow tangency condition on the airfoil surface. In the inverse-design procedure presented here, the pressure distribution rather than the airfoil coordinates is used as an input and our goal is to find the shape that an airfoil must have to achieve this input pressure distribution. Accordingly, for the inverse problem, neither a Neumann boundary condition for ϕ nor a Dirichlet boundary condition for ψ can be given on the airfoil surface since its location is unknown. This is in contrast to direct analysis methods where the airfoil geometry is known prior to the computational procedure. The problem of a prescribed pressure on a given airfoil is ill-posed.[7,20] Here we prescribe a general pressure distribution and find an airfoil that has a pressure distribution very close to a target pressure distribution.

The Hodograph Transformation

For two-dimensional irrotational flow, the nonlinear equations (7) for steady flow can be rendered linear by changing the role of the dependent and independent variables. We introduce the complex velocity

$$u - iv = qe^{-i\theta} \tag{9}$$

with u, v, q, and θ being functions of a complex variable

$$z = x + iy \tag{10}$$

We then have, using Eqs. (6) and (9) in differential notation,

$$d\phi + i(1/\rho)d\psi = (u - iv)(dx + i dy) = qe^{-i\theta} dz \tag{11}$$

and hence, with q and θ as independent variables, and since $\rho = \rho(|\nabla\phi|)$, we find

$$\left(\frac{\partial z}{\partial \theta}\right)_q = \frac{e^{i\theta}}{q}\left(\frac{\partial \phi}{\partial \theta} + i\frac{1}{\rho}\frac{\partial \psi}{\partial \theta}\right) \tag{12a}$$

$$\left(\frac{\partial z}{\partial q}\right)_\theta = \frac{e^{i\theta}}{q}\left(\frac{\partial \phi}{\partial q} + i\frac{1}{\rho}\frac{\partial \psi}{\partial q}\right) \tag{12b}$$

Differentiating Eq. (12a) with respect to θ and Eq. (12b) with respect to q and then equating the real and imaginary parts, we obtain the hodograph equations, viz.,

$$\frac{\partial \phi}{\partial \theta} = \frac{q}{\rho}\frac{\partial \psi}{\partial q}$$

$$\frac{\partial \phi}{\partial q} = -\frac{1}{\rho q}(1 - M^2)\frac{\partial \psi}{\partial \theta} \tag{13}$$

In the present design procedure, it is essential to introduce the Prandtl-Meyer function ν, defined by

$$\nu = \int_{q^*}^{q} \sqrt{|1 - M^2|}\,\frac{dq}{q} \tag{14}$$

in place of the velocity q in Eqs. (13), which then take their canonical form and become

$$\phi_\theta = K(\nu)\psi_\nu, \qquad \phi_\nu = \pm K(\nu)\psi_\theta \tag{15}$$

Here the $\pm$ signs refer to supersonic and subsonic conditions, respectively, and

$$K(\nu) = K[\nu(M)] = [|1 - M^2|]^{1/2}/\rho[q(M)] \tag{15a}$$

A typical physical and hodograph plane representation (with ν and θ as hodograph variables) of the flowfield is sketched in Fig. 1. The airfoil maps into a closed curve containing the stagnation point S at infinity. The region of the flow in Fig. 1a, bounded by the dotted contour and the airfoil,

represents a region in which every point has a velocity and flow angle equal to that of some other point outside this region, e.g., $q_e = q_f$ and $\theta_e = \theta_f$. Therefore points e and f will correspond to the same point in the hodograph plane, which must be considered as a Riemann surface of two sheets with a branch cut (lines dn and cn) connecting them. The local nature of this flow was studied by Lighthill[21] in his hodograph study of compressible flows past lifting airfoils.

Because the governing equations (15) are linear in the hodograph plane, there is usually no particular difficulty in finding solutions to them, by numerical methods if necessary. However, the presence of the second sheet of the two-sheeted Riemann surface and the a priori unknown location of the airfoil surface represent major obstacles in solving the governing equations in this plane. From Eqs. (15) it can be shown that the second-order derivatives for both ν and θ form the Laplacian or the wave operator, depending on whether or not the flow is subsonic or supersonic. Thus the equations for the subsonic flow are invariant in their general form under a conformal transformation.

Procedure

We proceed by assuming that there exists a conformal map of the subsonic portion of the two-sheeted Riemann surface of Fig. 1b into the unit circle of Fig. 2. (The double-connected infinite domain may be mapped into a finite, simply connected domain through an exponential mapping followed by a square root mapping to unfold the Riemann sheets.) Here the boundary of the unit circle corresponds to the airfoil surface wetted by subsonic flow. Because Bernoulli's equation, viz.,

$$\frac{1}{2}q^2 + \int \frac{dp}{\rho} = \text{const}$$

provides a correspondence between the values of p and the local sound speed, we may formulate the inverse design problem in terms of either M or p, and our choice of M is only a matter of convenience. A typical choice of M for a subcritical airfoil with a cusped trailing edge is illustrated in Fig. 3.

With the Mach number given on the boundary of the unit circle and with the subsonic portion of the flow inside the circle, we take advantage of the fact that the mapping to the ξ_0 plane is conformal. Thus, the Prandtl-Meyer function ν and the flow deflection angle θ are conjugate harmonics, i.e.,

$$F(\xi_0) = \nu + i\theta$$

or

$$\nabla^2 \nu(\xi_0) = 0 \tag{16}$$

$$\nabla^2 \theta(\xi_0) = 0 \tag{17}$$

Here $F(\xi_0)$ is the mapping function and $\xi_0 = re^{i\omega}$, with r and ω being the radial and angular coordinate measured in the ξ_0 plane. Boundary conditions for Eq. (16) are provided through the use of Eq. (14) relating ν and M; that is, knowing the Mach number distribution on the unit circle, we calculate ν employing Eq. (14). We then solve Laplace's equation for ν inside the unit circle using Fourier series, which determines the flow deflection angle θ to within a constant. However, the Prandtl-Meyer function ν is logarithmically singular in $q[\nu \propto \log(q)]$ at the stagnation point S which, for convenience, is positioned at $\xi_0 = -1$ in the ξ_0 plane. Therefore, in order to solve the boundary value problem for ν with Fourier series, we need first to subtract the logarithmic behavior at point S. This is done as follows:

Let

$$\bar{F}(\xi_0) = F(\xi_0) - \log(\xi_0 + 1)$$

$$G(\xi_0) = \nu(\xi_0) - \mathrm{Re}\{\log(\xi_0 + 1)\}$$

$$H(\xi_0) = \theta(\xi_0) - \mathrm{Im}\{\log(\xi_0 + 1)\}$$

then Eqs. (16) and (17) become

$$\nabla^2 G(\xi_0) = 0 \tag{18}$$

$$\nabla^2 H(\xi_0) = 0 \tag{19}$$

Here $\mathrm{Re}\{\ldots\}$ and $\mathrm{Im}\{\ldots\}$ are the real and imaginary parts of $\log(\xi_0 + 1)$, respectively. Equation (18) is then solved inside the unit circle using the Fourier series subject to the following boundary condition:

$$G(r=1,\omega) = \nu(1,\omega) - \mathrm{Re}\{\log(e^{i\omega} + 1)\}$$

Having obtained the solution for $G(r,\omega)$ in the unit circle, we then add back the logarithmic singularity to preserve the singular behavior of ν at the stagnation point.

Reformulating the definitions for the partial derivatives in Eqs. (15) in terms of r and ω, we obtain

$$\phi_r = -(1/r)K(\nu)\psi_\omega \tag{20a}$$

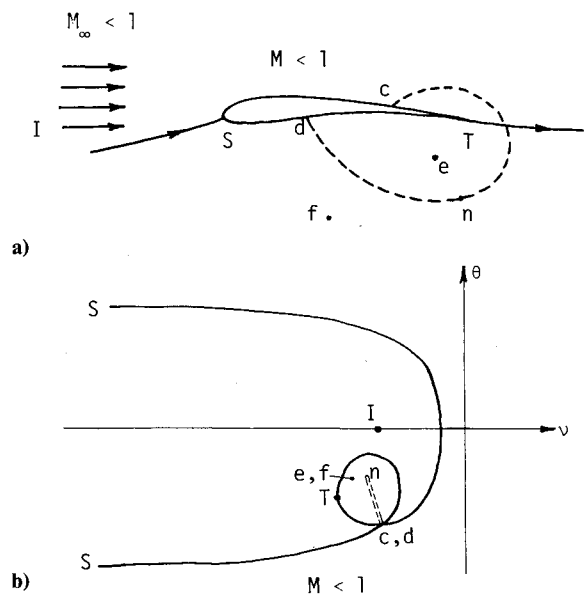

Fig. 1 Airfoil and its hodograph representation: a) subsonic flow past a lifting airfoil (stagnation point S, trailing edge T, far field I, and branch point n); b) hodograph representation of the flowfield shown in Fig. 1a.

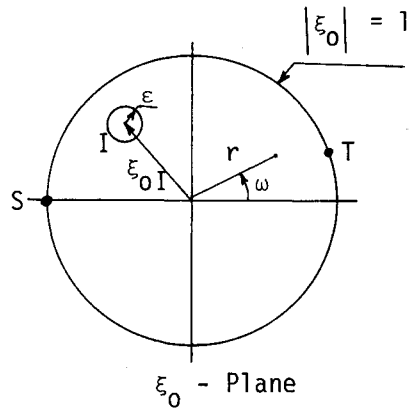

Fig. 2 Airfoil boundary in the ξ_0 plane (stagnation point S, trailing edge T, far field I).

and

$$\phi_\omega = rK(\nu)\psi_r \tag{20b}$$

Equations (20) can be reduced to a single equation in either ϕ or ψ. Eliminating ϕ through cross differentiation of Eqs. (20), we find the equation for ψ

$$r^2\psi_{rr} + r\psi_r + \psi_{\omega\omega} = f(M)\{r^2\nu_r\psi_r + \nu_\omega\psi_\omega\} \tag{21}$$

Here K is a function of M through Eq. (15a), M is a function of ν through Eq. (14), and

$$f(M) = -\left(\frac{\gamma+1}{2}\right)M^4(1-M^2)^{-3/2} \tag{21a}$$

Equation (21) is the ξ_0 plane counterpart of the physical plane in Eq. (7) for the stream function. The transformation to hodograph variables ν and θ, followed by a conformal transformation to the ξ_0 plane results in a linear second-order partial differential equation for ψ. In addition to this linearity, the major advantages of these two transformations are the unfolding of the two-sheeted hodograph surface to a single sheet and the representation of the subsonic boundary of the unknown airfoil by a unit circle. But these advances are not without attendant complexities, albeit minor ones. These difficulties include the presence of point I in Fig. 2, representing the far field inside the unit circle, at which the stream function is singular, and the singularity in $f(M)$ in Eq. (21a) at $M=1$. The first of these minor difficulties is circumvented through a coordinate transformation of the ξ_0 plane into the ξ plane sketched in Fig. 4. The transformation employed is the bilinear transformation which has the form

$$\xi = \acute{r}e^{i\acute{\omega}} = \left(\frac{A+B\xi_0}{C+D\xi_0}\right)e^{-i\beta} \tag{22}$$

where

$$A = \xi_{0_I}(\bar{\xi}_{0_I} - 1), \qquad B = \bar{\xi}_{0_I}(1-\xi_{0_I})$$

$$C = (\bar{\xi}_{0_I} - 1), \qquad D = (1-\xi_{0_I})$$

With $\acute{r}$ and $\acute{\omega}$ as new independent variables, the governing equation for ψ becomes

$$\acute{r}^2\psi_{\acute{r}\acute{r}} + \acute{r}\psi_{\acute{r}} + \psi_{\acute{\omega}\acute{\omega}} = f(M)\{\acute{r}^2\nu_{\acute{r}}\psi_{\acute{r}} + \nu_{\acute{\omega}}\psi_{\acute{\omega}}\} \tag{23}$$

In Eq. (23) the quantities $\nu_{\acute{r}}$ and $\nu_{\acute{\omega}}$ are evaluated through the utilization of the solution obtained for Eq. (16) in conjunction with Eq. (22). That is,

$$\nu_{\acute{r}} = \frac{1}{\acute{r}}\mathrm{Re}\{\xi\acute{F}(\xi)\}, \qquad \nu_{\acute{\omega}} = -\mathrm{Im}\{\xi\acute{F}(\xi)\}$$

where

$$\acute{F}(\xi) = e^{-i\omega}\left(\nu_r - \frac{i}{r}\nu_\omega\right)\frac{BC+DA}{(B-D\xi_0 e^{i\beta})^2}e^{i\beta}$$

Boundary Conditions

On the airfoil surface wetted by subsonic flow we have

$$\psi(1,\acute{\omega}) = 0 \qquad 0 \geq \acute{\omega} \geq 2\pi$$

The compressible far-field stream function ψ_∞ is related to its incompressible counterpart Ψ_∞ by

$$\psi_\infty = \frac{1}{K(\nu_\infty)}\Psi_\infty$$

$$= \frac{1}{K(\nu_\infty)}\mathrm{Im}\left\{\frac{q_\infty e^{i\alpha}}{(\xi_0 - \xi_{0_I})} - \frac{i\Gamma}{2\pi}\log(\xi_0 - \xi_{0_I})\right\} \tag{24}$$

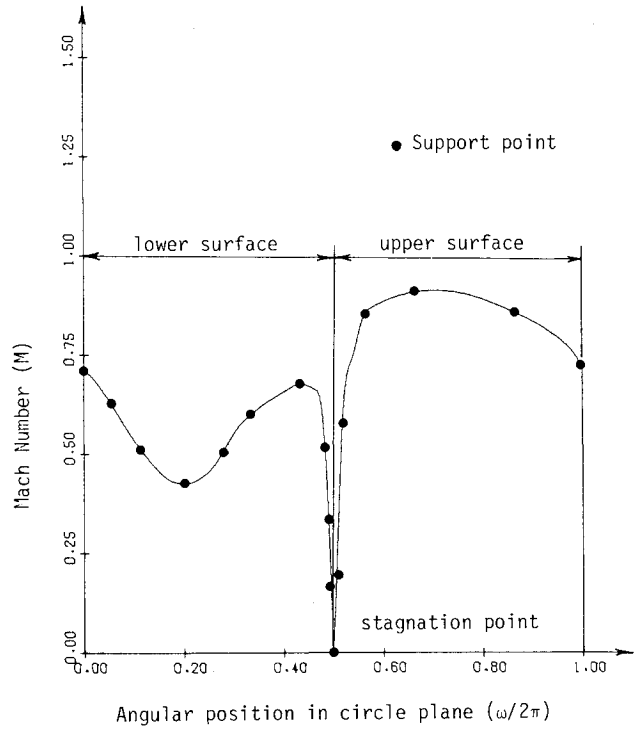

Fig. 3 Typical input Mach number distribution (the location of the trailing edge T is not known in advance).

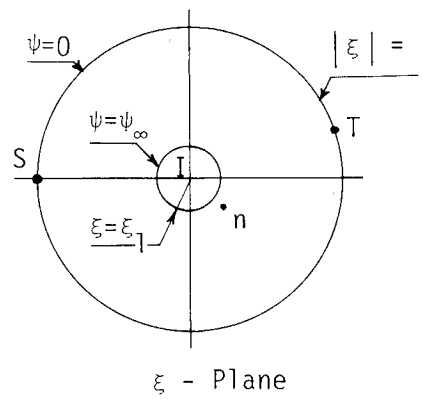

Fig. 4 Airfoil boundary in the computational plane (stagnation point S, trailing edge T, far field I, branch point n).

Equation (24) is a consequence of the fact that, at point I, which represents infinity in the ξ_0 plane, Eqs. (20) reduce to the familiar Cauchy-Riemann equations (or incompressible flow equations) expressed in polar coordinates. Thus, the complex potential defining the far-field stream function is that for an incompressible flow Ψ_∞ which is related to its compressible counterpart ψ_∞ through Eq. (24). In conjunction with Eq. (22), Eq. (24) is the employed in expressing the far-field boundary conditon in the ξ plane.

The boundary value problem for the stream function is now complete and Eq. (23) is then solved iteratively using a sixth-order accurate fast Poisson solver devised by Roache.[22] The stagnation streamline leaves the contour of an airfoil at a cusped or wedged trailing edge. In direct analysis, this defines the amount of circulation around the airfoil and the location of the stagnation point near the leading edge. For an indirect method such as the present one, the situation is exactly the reverse: since the (mapped) stagnation point location is given, we have to vary the circulation until the stagnation streamline reaches the surface perpendicular to the airfoil at the

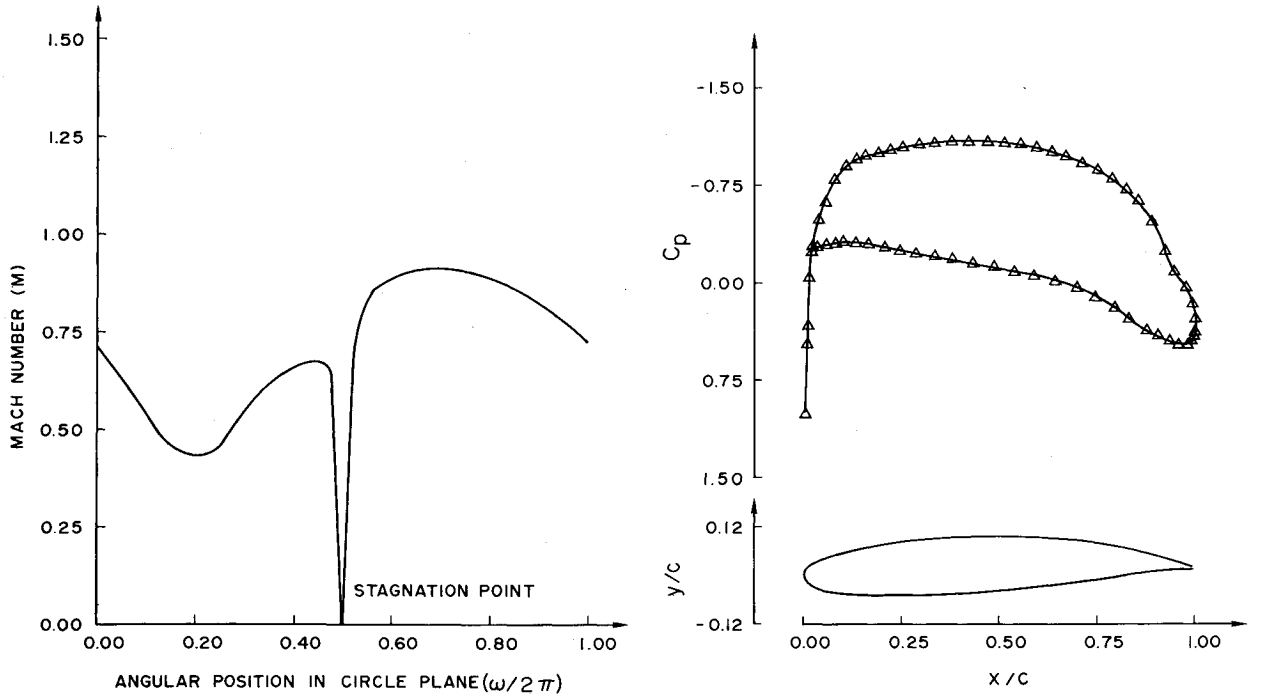

Fig. 5 Airfoil 819259 ($M_\infty = 0.589$, $C_L = 0.7493$, $C_D = 0.0001$, AOA = 1.281 deg).

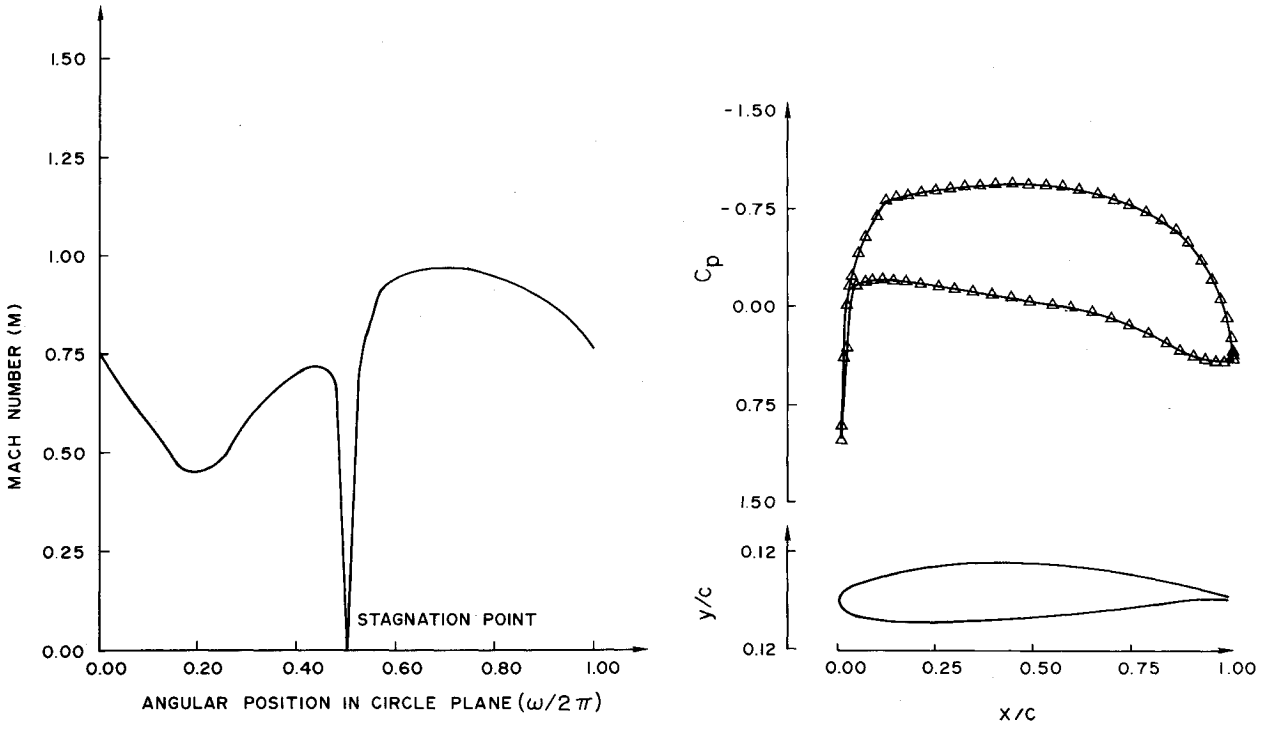

Fig. 6 Airfoil 809762 ($M_\infty = 0.622$, $C_L = 0.7984$, $C_D = 0.0001$, AOA = 1.027 deg).

stagnation point. It is noteworthy to mention here that the amount of circulation necessary to satisfy the normality condition of the front stagnation streamline is always consistent with that calculated using a contour integral of the velocity around the resulting airfoil. The mapped location T of the trailing edge results from this adjustment and the trailing-edge shape is then cusped. In the computational plane, the stagnation streamline leaves the airfoil contour at T at a 90 deg angle.

The results for the gradients ψ_ν and $\psi_{\acute{\omega}}$ along the elliptic boundary are then utilized in finding the inverse map to the physical plane [Eq. (11)], which can be written as

$$dx(\acute{\omega}) = \frac{1}{q}\left\{K(\nu)\cos(\theta)\psi_\nu - \frac{1}{\rho}\sin(\theta)\psi_{\acute{\omega}}\right\}d\acute{\omega} \tag{25a}$$

and

$$dy(\acute{\omega}) = \frac{1}{q}\left\{K(\nu)\sin(\theta)\psi_\nu + \frac{1}{\rho}\cos(\theta)\psi_{\acute{\omega}}\right\}d\acute{\omega} \tag{25b}$$

Equations (25) are numerically integrated along the unit circle starting from the trailing edge T on th airfoil's lower surface

moving toward the stagnation point S and finally ending at the trailing edge T on the airfoil's upper surface, i.e.,

$$x = x_0 + \int_{\acute{\omega}_T}^{2\pi+\acute{\omega}_T} dx(\acute{\omega}) \tag{26a}$$

$$y = y_0 + \int_{\acute{\omega}_T}^{2\pi+\acute{\omega}_T} dy(\acute{\omega}) \tag{26b}$$

The resulting airfoil configuration is then checked to see if it has a reasonable thickness distribution. If it does not, the input design parameters must then be altered and the design procedure repeated.

Computer Program Package

The computer program package consists of 15 FORTRAN IV subroutines performing calculations and data transfer. The package makes use of two permanent files, one for the results to be retained and one for input data.

For a specific airfoil design, the program has to be operated in the following manner:

1) Using the input Mach number distribution (which must be reasonable) in addition to the two specific design parameters M_∞ and α, we obtain a subsonic boundary configuration and have it displayed on a computer terminal with graphic capabilities. The configuration obtained is usually that of an airfoil with a relatively large x gap at the trailing edge. This gap is interactively reduced as explained in step 2.

2) The level of the input Mach number distribution on the lower surface ($0 < \omega < \pi$) is moved slightly in order to shift the location of the far-field singularity in the computational plane. This is in turn sufficient to reduce the x gap of the trailing edge of the resulting configuration to a preset value (e.g., 10^{-3}). The outcome of this step is an airfoil configuration with a small x gap at the trailing edge and a y gap that is also reduced interactively as explained in step 3.

3) The input Mach number distribution is then altered in the vicinity of the stagnation point of the resulting configuration to reduce the y gap at that point.

Results

In this section, a number of numerical results are presented and some experience with the algorithm is discussed. A few examples of airfoil designs are presented in Figs. 5 and 6. The airfoils cover a range of freestream Mach numbers and lift coefficients. A comparison with results obtained from the direct computation of the flowfield utilizing the designed airfoil geometries as input is also illustrated in Fig. 7 for subcritical airfoils. The analysis code FL06, devised by Jameson,[6] utilizes a finite difference method to solve the governing equations iteratively after mapping the airfoil into the unit circle.

For the design of subcritical airfoils with cusped trailing edges, Figs. 5 and 6 illustrate the different input Mach number distributions required for the design procedure and the resulting airfoil shapes at $M_\infty = 0.589$ and 0.622. Through a study of these airfoils we have demonstrated that small modifications in the input Mach number distribution near the stagnation point have a substantial influence on the y gap at the airfoil trailing edge and, hence, on airfoil closure. That is, increasing the slope of the Mach number distribution at the stagnation point results in an airfoil with a smaller nose radius and consequently a smaller thickness-to-chord ratio, which ultimately results in a smaller y gap at the airfoil trailing edge. Experience has shown that, in the process of minimizing the y gap at the trailing edge, the level of the input Mach number distribution has to be altered on the lower or upper surface, or both, to maintain the x gap at a present value, e.g., 10^{-3}.

Figure 7 compares the results obtained from analysis computation of the flowfield utilizing the designed airfoil geometries shown in Figs. 5 and 6 as input. Results obtained from both the design and the analysis show good agreement except near the trailing edge.

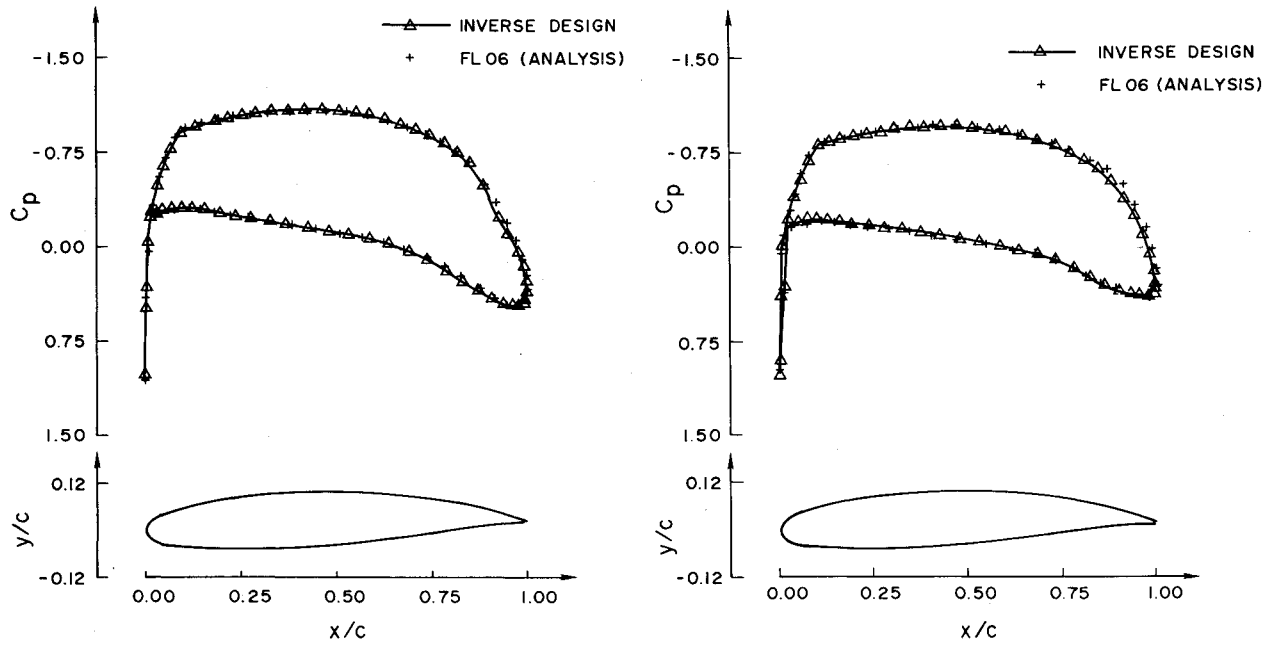

a) Airfoil 819259

	Inverse	FL06
M_∞	0.589	0.589
C_L	0.7493	0.7493
C_D	0.0001	0.0000
AOA, deg	1.281	2.560

b) Airfoil 809762

Inverse	FL06
0.622	0.622
0.7984	0.7984
0.0001	0.0000
1.027	3.214

Fig. 7 Pressure coefficient distribution comparison.

Conclusion

Based on hodograph theory, an efficient design procedure has been developed that can be used for the aerodynamic design of subcritical airfoil sections. An analysis of the numerical solutions obtained with this design procedure indicates that only one airfoil configuration is obtained for a desired input target pressure and freestream flow conditions. Experience has also shown that the input Mach number distribution (or pressure) and the freestream Mach number cannot be prescribed independently of each other if a practical airfoil configuration is sought. That is, for a solution to exist for the design problem we have two alternatives: 1) fix the freestream Mach number and alter the pressure or 2) vary the freestream Mach number and fix the pressure. The former alternative, used in the present study, is more practical from the designer's point of view where his primary interest lies in finding an airfoil section suitable for a specific flight Mach number. Subcritical airfoils with a target pressure can be found with modest effort when the algorithm is in the hands of an experienced user.

Within the framework of our design procedure it seems possible that the procedure can be extended further to study a large class of aerodynamically interesting airfoils (shock-free supercritical airfoils) and their corresponding pressure distributions. Moreover, while the results are given for inviscid flow, the same procedure can be employed iteratively with a boundary-layer calculation (utilizing airfoils with an open trailing edge) in order to achieve viscous airfoil designs.

From the engineering point of view, the method was found to be sufficiently accurate and flexible in providing results at moderate cost. Indeed, less than a minute of CYBER 175 CPU time is required to design a subcritical airfoil section.

Acknowledgment

This research was carried out by the Computational Mechanics Laboratory at the University of Arizona, Department of Aerospace and Mechanical Engineering. The work was supported by AFOSR Grants 76-2954 and 81-0107 and ONR Grant N0001476-C-0182, P0006.

References

[1]Stratford, B. S., "The Prediction of Separation of the Turbulent Boundary Layer," *Journal of Fluid Mechanics*, Vol. 5, July 1959, pp.1-16.

[2]Goldstein, S., "A Theory of Aerofoils of Small Thickness, Part III—Approximate Designs of Symmetrical Aerofoils for Specified Pressure Distributions," Aeronautical Research Committee, London, Rept. ARC 6225, Oct. 1942.

[3]Sells, C. C. L., "Plane Subcritical Flow Past a Lifting Airfoil," Royal Aircraft Establishment, London, Rept. RAE-TR-67146, 1964.

[4]Murman, E. M. and Cole, J. D., "Calculation of Plane Steady Transonic Flows," *AIAA Journal,* Vol. 9, 1971, p. 114-121.

[5]Garabedian, P. R. and Korn, D. G., "Analysis of Transonic Airfoils," *Communications on Pure and Applied Mathematics,* Vol. 24, 1976, pp. 369-382.

[6]Jameson, A., "Iterative Solution of Transonic Flows Over Airfoils and Wings, Including Flows at Mach 1,"*Communications on Pure and Applied Mathematics,* Vol. 27, 1974, pp. 283-309.

[7]Volpe, G. and Melnik, R. E., "The Role of Constraints in the Inverse Design Problem for Transonic Airfoils," AIAA Paper 81-1233, June 1981.

[8]Lighthill, M. J., "A New Method of Two-Dimensional Aerodynamic Design," Aeronautical Research Council, London, R&M 2112, April 1945.

[9]Tranen, T. L., "A Rapid Computer Aided Transonic Airfoil Design Method," AIAA Paper 74-501, June 1974.

[10]Nixon, D., "Perturbation of a Discontinous Transonic Flow," *AIAA Journal,* Vol. 16, Jan. 1978, pp. 47-52. (Also see NASA TM-78521 and AIAA Paper 79-0076, 1979.)

[11]Hicks, R. M. and Vanderplaats, G. N., "Application of Numerical Optimization to the Design of Supercritical Airfoils without Drag Creep," SAE Paper 770440, March 1977.

[12]Davis, W. M., "Techniques for Developing Design Tools from the Analysis Methods of Computational Aerodynamics," AIAA Paper 79-1529, July 1979.

[13]Haney, H. P. and Johnson, R. R., "Application of Numerical Optimization to the Design of Wings with Specified Pressure Distributions," NASA CR 3238, Feb. 1980.

[14]Hicks, R. M. and Henne, P. A., "Wing Design by Numerical Optimization," AIAA Paper 77-1247, 1977.

[15]Niewland, G. Y., "Transonic Potential Flow Around a Family of Quasi-Elliptical Aerofoil Sections," National Aerospace Laboratory NLR, the Netherlands, Rept. NLR-TR-T172, 1967.

[16]Bauer, F., Garabedian, P., and Korn, D., "Supercritical Wing Sections III, "*Lecture Notes in Economics and Mathematical Systems,* Springer Verlag, New York, 1977.

[17]Boerstoel, J. W. and Huizing, G. H., "Transonic Shock-Free Airfoil Design by an Analytical Hodograph Method," AIAA Paper 74-539, 1974.

[18]Sobieczky, H., "Related Analytical, Analog, and Numerical Methods in Transonic Airfoil Design, AIAA Paper 79-1556, July 1979.

[19]Sobieczky, H., "Entwurf uberkritisher Profile mit Hilfe der Rheoelectrischen Analogic," DFVLR-AVA, Göttingen, FRG, DF-VLR Rept. DLR-FB 75-43, 1975.

[20]Thwaites, B., *Incompressible Aerodynamics: An Account of the Theory and Observation of the Steady Flow of Incompressible Fluid Past Aerofoils, Wings and Other Bodies,* Clarendon Press, Oxford, England, 1960, p. 138.

[21]Lighthill, M. J., "On the Hodograph Transformation for High Speed Flow," *Quarterly Journal of Mechanics and Applied Mathematics,* Vol.1, 1948, pp. 442-450.

[22]Roache, P. J., "Sixth Order Accurate Direct Solver for the Poisson and Helmholtz Equations," *AIAA Journal,* Vol. 17, May 1978, pp. 524-526.